Detumbling an Uncontrolled Satellite with Contactless Force by Using an Eddy Current Brake

Fumihito Sugai, Satoko Abiko, Teppei Tsujita, Xin Jiang, and Masaru Uchiyama

Abstract— In this paper we propose a new method to detumble a malfunctioning satellite. Large space debris such as malfunctioning satellites generally rotates with nutational motion. Thus several researches have proposed the methods to use a space robot for capturing and deorbiting these debris. The most of the past studies considered the method to detumble an uncontrollable satellite and then capture a single spinning satellite. However these methods require physical contact with malfunctioning satellites, which has a risk of accident. Therefore, we propose a method with an eddy current brake [1]. The eddy current brake system can produce braking force to the target without any physical contact. Thus, we can reduce the risk of critical collision between the space robot and the target object. This paper firstly reviews dynamics of a tumbling satellite and proposes a detumbling strategy with the eddy current brake. We carry out a fundamental experiment to evaluate the performance of the braking force of the developed eddy current brake system, and then we simulate detumbling operation by using the experimental data and show an effectiveness of the proposed detumbling method.

I. INTRODUCTION

Recently a lot of space debris exist in the earth orbit. These debris have been considered to become the obstacles of current and future space activities. The debris have been generated due to the past and current space missions and consist of, for example, rocket stages, malfunctioning satellites, and so on. Among them, large debris such as malfunctioning satellites have high risk of colliding with ongoing operational spacecrafts or any other debris. As a result of collision with large space debris, a big amount of small debris is scattered in the orbit. In fact, such an accidental collision was happened in 2009 and tons of debris have been dispersed around the earth [2]. Hence, many researchers have studied the ways for space robots to deorbit large debris such as the malfunctioning satellites safely.

To achieve deorbiting the malfunctioning satellites by the space robots, there are three elemental technologies; rendezvous, capturing, and deorbiting. In these elemental technologies, rendezvous and deorbiting technologies have been verified or are in the process of verification in orbit [3]–[6]. On the other hand, although many methods have been proposed for capturing the target satellite, there is no absolute reliable solution since it involves risk to have a contingent collision. Therefore the past proposed methods have been verified by only numerical simulation or ground facilities.

F. Sugai is with Department of Mechanical Systems and Design, Graduate School of Engineering, Tohoku University, 6-6-01 Aramakiaza-Aoba, Aoba-ku, Sendai 980-8579, Japan. {sugai, abiko, tsujita, jiangxin, uchiyama}@space.mech.tohoku.ac.jp

In general, the malfunctioning satellites are considered to be out of control due to the loss of the attitude control and they rotate with nutational motion. In fact, the motion of several uncontrolled satellites have been observed from the earth [7]. Key technologies to capture such uncontrollable satellites are how to deal with relative rotational motion between the target and the space robot and how to capture it safely without critical hard contact. In several related researches [8], [9], they assume that the space robot can follow suitable trajectory which achieves zero relative velocity between the capturing point of the target and the robot. However it is not easy to achieve zero relative velocity between the space robot and the target due to complex motion of the target and the limited movable area of the space robot. If there exists non-zero relative velocity, contingent contact would happen and lead to the destruction of the robot arm or the target, or the target satellite would be bounced away. In [10], [11], they proposed the method that the space robot firstly detumbles (making nutational motion to single spin motion) a nutational motion of the target satellite, and then captures the target. This approach is more practical to capture the target since it is simpler to track certain point to grasp even when the target does not have a dedicated grasping point in the single spin motion. However this method still has a drawback of physical contact in the process of the detumbling.

To reduce a risk of the hazardous contact between the target and the space robot, we propose a new method for detumbling an uncontrolled target without any physical contact by using an eddy current brake. Up to now, we developed an eddy current brake system and evaluated the performance of the first prototype brake system [1]. In this paper first briefly reviews dynamics of a tumbling object and proposes a detumbling strategy by using the developed eddy current brake system. Then, we carry out a fundamental experiment to evaluate the performance of the braking force of the developed eddy current brake system. Finally we simulate a detumbling operation by using the experimental data and verify an effectiveness of the proposed detumbling method.

II. DYNAMICS OF A TUMBLING SATELLITE AND A DETUMBLING STRATEGY

This section firstly explains a tumbling motion of the target satellite. Then we propose a strategy of detumbling an uncontrollable satellite by using the eddy current brake.

A malfunctioning satellite generally loses its attitude control and rotates freely. Firstly let us consider, for simplicity, motion of a spinning satellite whose moment of inertia is
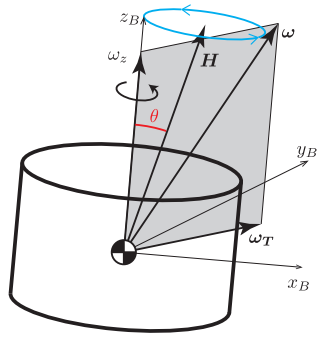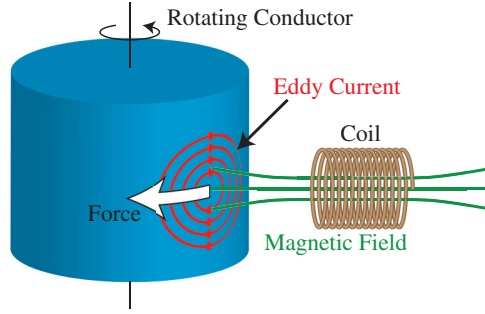
Fig. 1.   Nutational motion.
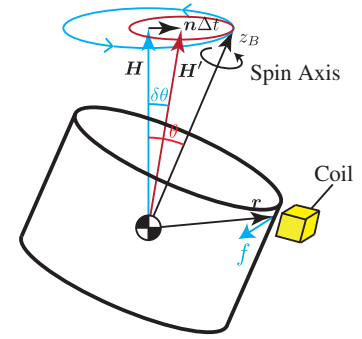

Fig. 2.   Principle of an eddy current brake.

Fig. 3.   Precession by an eddy current brake.

$I = \mathrm{diag}[I_x, \ I_y, \ I_z] = \mathrm{diag}[I_T, \ I_T, \ I_s]$. Assuming that angular momentum and angular velocity of the satellite are H and ω respectively, the equation of motion of the satellite is expressed by the following Euler equation of a rigid body.

$$\frac{d\boldsymbol{H}}{dt} + \boldsymbol{\omega} \times \boldsymbol{H} = \boldsymbol{M}. \tag{1}$$

where M is torque. and z axis is considered as the spin axis of the satellite. When the satellite is not subjected to external torque, M becomes zero. Substituting a moment of inertia $I = \mathrm{diag}[I_T, \ I_T, \ I_s]$ and $\boldsymbol{\omega} = [\omega_x \ \omega_y \ \omega_z]^T$ to the above equation, the following equation is derived.

$$\left. \begin{array}{rcl} I_T\dot{\omega}_x & + & (I_s - I_T)\omega_y\omega_z & = & 0 \\ I_T\dot{\omega}_y & + & (I_T - I_s)\omega_z\omega_x & = & 0 \\ I_s\dot{\omega}_z & & & = & 0 \end{array} \right\}. \tag{2}$$

From the third equation, the spin rate ω_z is constant. The first and second equations are expressed as follows:

$$\left. \begin{array}{rcl} \dot{\omega}_x & + & \lambda\omega_y & = & 0 \\ \dot{\omega}_y & - & \lambda\omega_x & = & 0 \end{array} \right\}, \tag{3}$$

$$\lambda = \frac{I_s - I_T}{I_T}\omega_z. \tag{4}$$

From these equations, angular velocity $\boldsymbol{\omega}_T = \omega_x\hat{\boldsymbol{x}}_B + \omega_y\hat{\boldsymbol{y}}_B$ rotates around spin-axis with angular velocity λ in a direction perpendicular to spin axis. $\hat{\boldsymbol{x}}_B$ and $\hat{\boldsymbol{y}}_B$ denote unit vector along each axis.

In this dynamic motion, $\boldsymbol{\omega}$, $\boldsymbol{H}$, and $\hat{\boldsymbol{z}}_B$ (unit vector along z_B axis) lie in the same plane. When a spin satellite is not applied external force, an angular momentum $\boldsymbol{H}$ is constant. Therefore spin axis z_B rotates around $\boldsymbol{H}$ with maintaining a certain amount of angle between z_B and $\boldsymbol{H}$ (Fig. 1). This rotational motion is called nutational motion and that angle is called nutational angle θ.

In order to detumble a nutational motion of the target satellite, we have to add an external torque so as to making nutational angle decreasing. The external torque vector has to be a vector which lies in the same plane of angular momentum vector and spin-axis. Direction of the external torque vector has to be a direction from the angular momentum vector to the spin-axis.

In this detumbling strategy, we use an eddy current brake in order to exert a force to the target. In this paper, we assume that the eddy current brake system is attached on the tip of a robotic arm on a space robot. Fig. 2 shows a principle

of the eddy current brake. When a conductive object has a relative velocity to a magnetic field, an eddy current is generated so as to disturb changing a magnetic field. Thus, the rotating object is exerted by an interaction force between the eddy current and magnetic field so as to brake a rotating conductive object. The structure of most of satellites is made by nonmagnetic material such as aluminum alloy. Therefore the eddy current brake is feasible as to exert a braking force to the target satellites.

As shown in Fig. 3 a coil of the eddy current brake is placed near by the target. The coil applied a force $\boldsymbol{f}$ to brake a spinning motion. By applying a force $\boldsymbol{f}$ angular momentum $\boldsymbol{H}$ is precessed (changing an angular momentum with external torque) and the nutational angle θ changed with $\delta\theta$ as the following equation.

$$\delta\theta = \cos^{-1}\frac{\boldsymbol{H} \cdot \boldsymbol{H}'}{|\boldsymbol{H}||\boldsymbol{H}'|}, \tag{5}$$

$$\boldsymbol{H}' = \boldsymbol{H} + \boldsymbol{n}\Delta t, \tag{6}$$

$$\boldsymbol{n} = \boldsymbol{r} \times \boldsymbol{f}. \tag{7}$$

where $\boldsymbol{r}$ is a vector from the center of mass of the target to the position where an external force is applied. $\boldsymbol{n}$ is the torque exerted to the target satellite and Δt is a time duration when the eddy current brake applies force to the target satellite. The eddy current brake generates braking force at the time when the surface of the target passes through the efficient area of a coil of the eddy current brake while keeping no contact between them. As shown in Fig. 3, the vector of the angular momentum, $\boldsymbol{H}$ becomes closer to the spin-axis, z_B and the nutational angle, θ decreases to zero.

Fig. 4 shows numerical simulation when one eddy current brake applies the braking force to the tumbling target. The figure shows trajectories of the tip of the spin axis and the vector of the angular momentum. In the simulation, initial angular momentum is along z axis and nutational angle is 30 [°]. A coil of the eddy current brake is placed near the target satellite at initial condition. As shown in the figure, the angular momentum is precessed by the external torque and the trajectory of the spin axis moves to $+x$ direction and circular path becomes smaller. However this strategy has a problem that a space robot gets a reaction force when a space robot has only one robot arm on which a coil of the eddy current brake is attached. Therefore in order to keep a relative position between a space robot and a target satellite, we use two coils of the eddy current brake and two coils
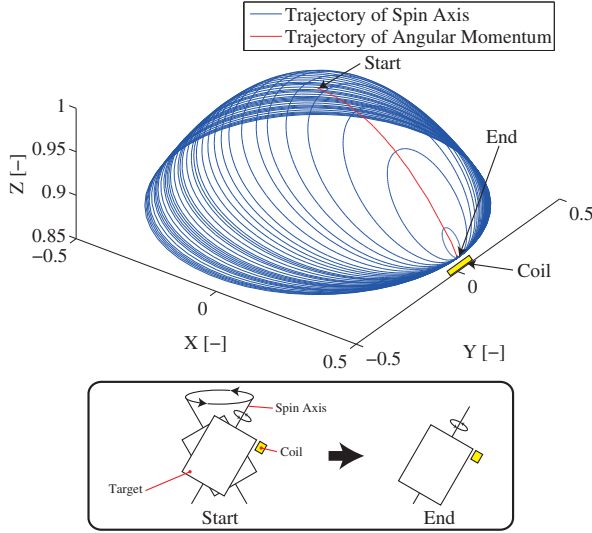
Fig. 4.   Trajectory of spin axis and angular momentum (using one coil).

Fig. 5.   Trajectory of spin axis and angular momentum (using two coils).

are placed opposite each other. These coils generate braking force to opposite direction and reaction forces are canceled out each other. Then, the space robot does not affect any reaction force and it gets only reaction torque.

Fig. 5 shows a simulation result of detumbling by two coils of the eddy current brake. By using two coils, angular momentum changes around initial direction in x axis, and center of the nutational motion does not move. Therefore the distance between the coils and the target gets longer. In order to keep the distance between the coils and the target, two coils have to move.

Fig. 6 shows a strategy of detumbling and capturing an uncontrolled satellite. The free-flying space robot has two arms, on which two coils of the eddy current brake are attached. Firstly the space robot moves two arms and approximates the coils to the target. Then the eddy current brake applies a braking force to the target in order to precess the motion of the target. At the same time the space robot control arms and keeps a distance between the coils and the target when nutation angle of the target gets smaller. Secondarily the eddy current brake reduces a spinning rate after the target motion becomes single spin. Finally the space robot captures the target satellite by two arms.

III. DEVELOPED EDDY CURRENT BRAKE & FUNDAMENTAL EXPERIMENT

We clarified the required specifications of the eddy current brake system and developed a linear induction motor typed eddy current brake system as shown in Fig. 7 and conducted fundamental experiment to measure a braking force of the developed eddy current brake [1]. In [1], we measured an output braking force to an aluminum flat plate as a target. The aluminum plate is fixed and the relative velocity between the coil of the eddy current brake and the plate is zero. In the actual detumbling mission, the target object is not a flat plate. In our assumption, the target has a curved surface and the relative velocity between the coil and the target object is not zero because the target object is tumbling.
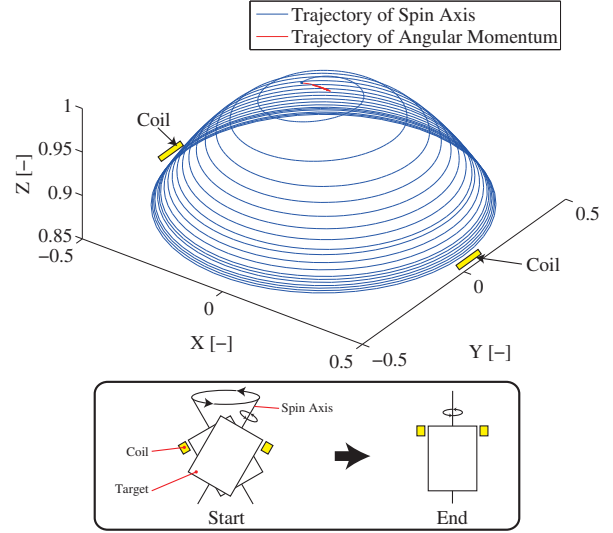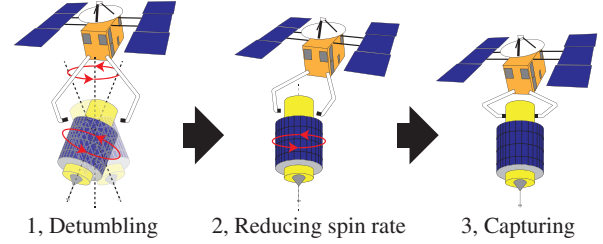

Fig. 6.   Strategy of detumbling and capturing a malfunctioning satellite.

In this section, first we measure braking force of the developed eddy current brake to an object that rotates around a single axis with constant angular velocity. Then we carry out experimental verification of the braking performance to a one-axis free rotating object.

A. Experiment 1: measuring braking force

1) Experimental setup: Fig. 8 shows an experimental setup. In the experiment, we use an acrylic cylinder as the target object, whose diameter was 400 [mm] and height was 90 [mm]. The target is placed on one axis spinning motion table. An aluminum plate, whose thickness was 2 [mm], was attached on outer surface of the acrylic cylinder. A coil of the eddy current brake is placed on the side of the cylindrical target with 5 [mm] gap. The coil is mounted on a force sensor and a braking force of the eddy current brake is measured by the force sensor.

We control a linear induction motor typed eddy current brake with a field oriented control(FOC). Fig. 9 shows a block diagram of FOC. We can control an output force directly by setting a reference of currents I_{dref} and I_{qref}. The magnitude of these currents correspond to the magnitude of magnetic field and torque, respectively. The FOC requires the relative velocity between the coil and the target. In actual operation, we need to measure a spinning rate of the target satellite. However in this experiment we predetermine constant angular velocity of the target and provide it to the controller in advance.

Furthermore, in this study, the plug braking approach is used, in which the direction of movement of the magnetic

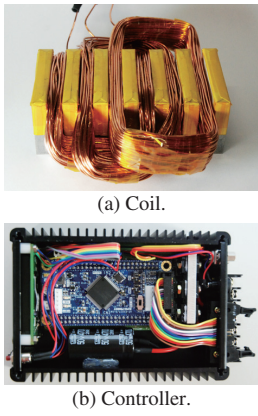(a) Coil.

(b) Controller.

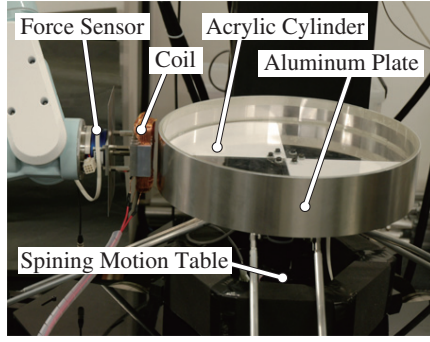Fig. 7. Overview of the eddy current brake system.
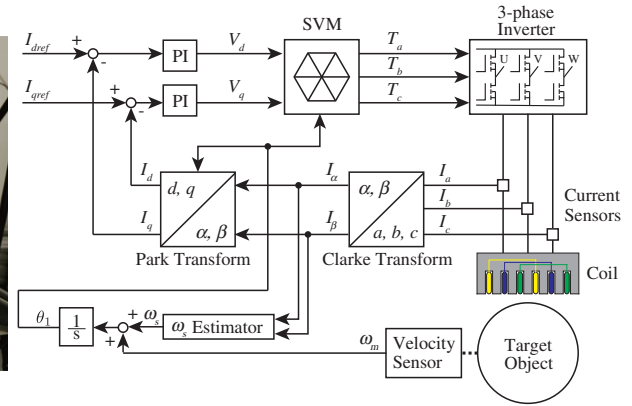

Fig. 8. Experimental setup.

Fig. 9. Block diagram of field oriented control.

field using the linear induction motor is inverse direction of the movement of the target. This method can provide large braking force when the relative velocity between the coil and the target is slow compared to the regenerating braking system.

In the experimental condition, the target object rotates four patterns of the angular velocity, namely $\{5\pi/6, 5\pi/3, 5\pi/2, 10\pi/3\}$ [rad/s]. We set two patterns of reference current: $I_{dref} = I_{qref} = \{5, 10\}$[A]. Then we measure braking force by the force sensor in each case.

2) Experimental result and remarks: Here firstly let us consider the relationship between the angular velocity of coil current ω_1, slip angular frequency ω_s and electric angular frequency ω_m which is obtained from the relative velocity as shown in (9).

$$\omega_1 = \omega_s + \omega_m, \tag{8}$$

$$\omega_m = \frac{2\pi v_m}{p}, \tag{9}$$

$$f = \frac{{\phi_2}^2}{r_2}\omega_s. \tag{10}$$

where v_m represents relative velocity between the coil and the target. Here we assume that the coil is fixed and the target is tumbling. Therefore, v_m can be expressed as follows:

$$v_m = \frac{d}{2}\omega_z \tag{11}$$

d and ω_z are a diameter and a spin rate of the target respectively. p is a pole pitch of the coil. f is an output force of the eddy current brake. r_2 [Ω] and ϕ_2 [Wb] denote resistance and interlinkage magnetic flux of the target object, respectively.

From the above equations, one can obtain the following relationship between the output force, f, and the angular velocity of the coil current, ω_1.

$$f = \frac{{\phi_2}^2}{r_2}(\omega_1 - \omega_m)$$
$$= \frac{{\phi_2}^2}{r_2}(\omega_1 - \frac{2\pi v_m}{p}). \tag{12}$$

Equation (12) implies that in order to provide constant braking force to the target, ω_1 should be determined larger

as the relative velocity is getting smaller. Therefore, higher voltage is required as the relative velocity gets smaller because inductive reactance becomes large. However power supply of the eddy current brake cannot supply required current due to the limitation of rated voltage. As a result, the braking force becomes smaller as the relative velocity gets slower.

In general, FOC determines the current for the output magnetic field and torque, I_{dref} and I_{qref}, as mentioned before, which indicates that the constant slip angular frequency, ω_s, is controlled to be constant. This approach is hereafter called as "Constant Braking Force". However, in the plug braking approach with FOC, one can actively use the effect of the relative velocity, ω_m while holding the angular velocity of the coil, ω_1, constant. In this case, the slip angular frequency, ω_s, gradually increases as the relative velocity gets larger which leads to the eddy current brake can generate larger braking force. This approach is hereafter termed as "Maximized Braking Force".

We conduct an experiment in order to verify how large the eddy current brake can provide larger braking force with the "Constant Braking Force(CBF)" approach and with the "Maximized Braking Force(MBF)" approach.

Fig. 10 shows an experimental result. In the case of $I_{dref} = I_{qref} = 5$[A] (CBF), braking force is approximately 0.06 [N] and maintained constant despite of the change of the angular velocity of the target. On the other hand, in the case of $I_{dref} = I_{qref} = 10$[A](CBF), the braking force gradually increases from 0.22 to 0.26 [N] when the angular velocity becomes large from $5\pi/6$ to $10\pi/3$ [rad/s]. This happened due to the limitation of the rated voltage as mentioned in the above. In Fig. 10, $I_{dref} = I_{qref} = 5$[A] (MBF) and $I_{dref} = I_{qref} = 10$[A] (MBF) show the experimental result of the "Maximized Braking Force" approach. The experimental result shows that in the case of the "Maximized Braking Force" approach, braking force becomes larger than the case of the "Constant Braking Force" approach.

Consequently, it is shown that the developed eddy current brake system can generate constant braking force despite of the change of the relative velocity in certain range of the current. But, more efficiently, the eddy current brake can generate larger force by using the relative velocity actively
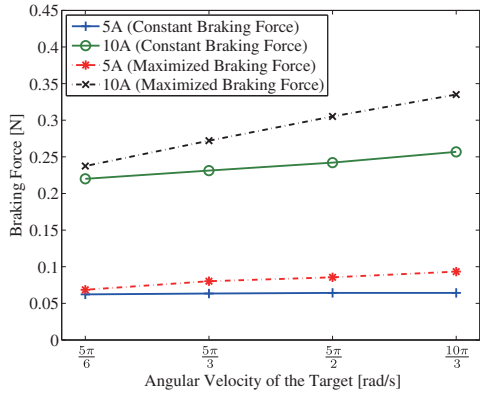
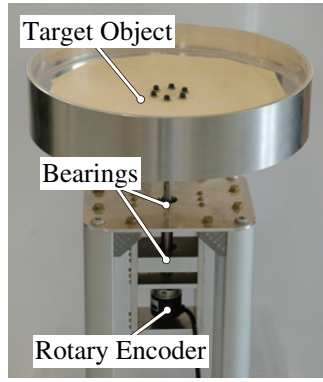Fig. 10. Experimental result.
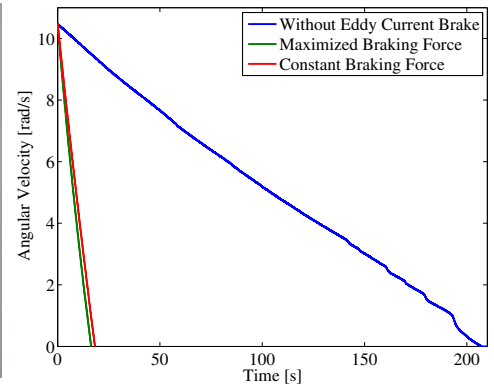

Fig. 11. Overview of a rotating table.

Fig. 12. Experimental result.

in plug braking.

B. Experiment 2: braking a free rotating object

From the result of experiment 1, it is shown that the eddy current brake system can work well for the constant relative velocity. However the relative velocity between the target and the coil generally varies due to the braking force. In this subsection, we verify if the eddy current brake can generate proper braking force during the decreasing of the relative velocity and finally the spinning motion of the object is stopped or not.

1) Experimental setup: A target object and a coil of the eddy current brake are same as in the experiment 1. The target is mounted on a free rotating table as shown in Fig. 11 which can rotate one-axis freely. A rotary encoder is attached on a rotating shaft and it measures an angle of the target object.

The angular velocity of the target when we start applying the braking force is $10\pi/3$ [rad/s]. We set a reference current $I_{dref} = I_{qref} = 10$[A]. We measure the angle of the target and the braking force during the angular velocity is from $10\pi/3$ to 0 [rad/s].

We carried out two patterns of braking approaches as mentioned in experiment 1, namely one is "Constant Braking Force" that feeds the relative velocity information back to the controller for keeping a braking force constant. Another one is "Maximized Braking Force" that makes braking force larger by passively using relative velocity. The "Constant Braking Force" approach sends the measurement data with the rotary encoder to the controller every 1 [s] to keep a constant braking force.

2) Experimental result and discussion: Fig. 12 shows an experimental result. By using the eddy current brake, the spin motion of the target converges to zero faster than the case without using any braking system. Comparing the case of "Constant Braking Force" with the case of "Maximized Braking Force", "Maximized Braking Force" can brake quicker than the other case. Fig. 13 shows a braking force in the case of "Maximized Braking Force" and "Constant Braking Force". The braking force in the case of "Maximized Braking Force" depends on the relative velocity. When the rotational speed of the target object is fast, the braking force is large and the braking force decreases as the rotational
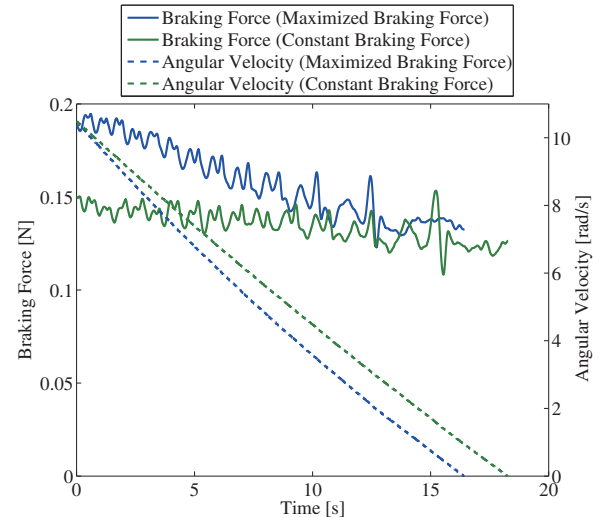

Fig. 13. Comparison of "Maximized" and "Constant" braking force.

speed gets slow. However, the "Maximized Braking Force" approach still can keep larger braking force than the case of "Constant Braking Force". On the other hand, in the case of "Constant Braking Force" the eddy current brake outputs constant braking force despite the rotational speed varies. But the magnitude of the output force is smaller than that of the "Maximized Braking Force" approach as mentioned before. In each case, there is cyclic jerk on the braking force. This is because an aluminum plate on the outer surface of the target object is not a perfect circle and the gap between the target object and the coil varies in a cycle.

As a result, the eddy current brake can apply braking force to the rotating target properly. By using the relative velocity data, it can generate constant braking force. Furthermore, it can generate larger braking force by making effective use of the relative velocity.

IV. DETUMBLING SIMULATION

In this section, we simulate detumbling operation for more realistic target with using the experimental result in Section III. As a target satellite, we assume a spinning satellite which is out of control and rotates with 100 [rpm] = $10\pi/3$ [rad/s] spin rate and 30 [°] nutation angle. The size of the target is assumed to be that of the climate satellite Himawari 5 whose mass is 345 [kg], diameter is 2.15 [m], and height is 3.54 [m].
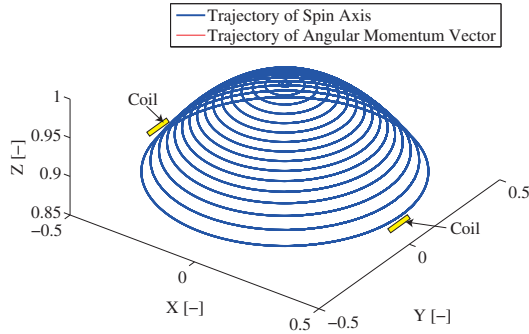
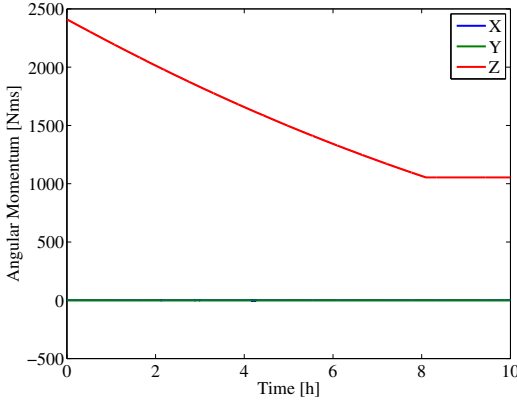Fig. 14. Trajectory of spin axis and angular momentum.

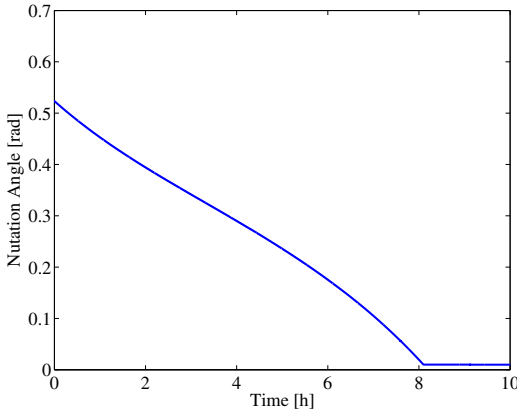Fig. 15. Angular momentum of the target satellite.

Fig. 16. Nutation angle of the target satellite.

However since we have no data about mass distribution, we set a simulation model as a homogenous cylindrical object and height of the model so as to make inertia ration 1.05 (this value is used as a design guide). Consequently, the height of the simulation model is 1.77 [m]. The moment of inertia is $I_S = 199$ [kg $\cdot$ m^2], $I_T = 190$ [kg $\cdot$ m^2] respectively. Initial attitude of the target satellite is set so as to align the direction of the angular momentum vector with z axis.

In the simulation, the coil of the eddy current brake is placed on the side of the target with 5 [mm] gap. The coil moves in order to keep the gap to the target constant when the target satellite is precessed. The eddy current brake applies the force at the moment when the target comes near the coil. The simulation will end if nutation angle will be less or equal 0.01 [rad].

Figs. 14 to 16 shows a simulation result. Fig. 14 shows

a trajectory of the tip of the spin axis and the angular momentum vector. The trajectory of the spin axis is plotting 5 [s] per half hour. From Fig. 14 the trajectory of the spin axis converges to a single spin motion, which means x and y becomes zero. Fig. 15 shows the angular momentum of the target satellite. This figure shows that x and y components of the angular momentum show little change around zero and at the same time z component of the angular momentum gets smaller. Fig. 16 shows nutation angle. From this figure, it is clearly shown that nutation angle becomes smaller while the eddy current brake system is applied to the target and finally the nutational motion converges to a single spinning motion

V. CONCLUSIONS AND FUTURE WORKS

In this paper we proposed a detumbling method using an eddy current brake system. We discussed detumbling dynamics and proposed a strategy for detumbling an uncontrollable satellite with two coils of the eddy current brake in order to cancel reaction force to the space robot. Then we carried out an experimental verification of the developed eddy current brake system to observe the generated braking force to the spinning target. Finally we simulated detumbling motion using the data of experimental verification and showed the efficiency of the proposed method.

In the future works, we will carry out an experiment of detumbling a target which rotates in 3 degrees of freedom. Besides, we will simulate detumble mission including an attitude control of a space robot itself and control of robot arm mounted on the space robot. After fundamental research is finished, we will study toward practical use of this detumbling method.

REFERENCES

[1] F. Sugai, et al., "Development of an Eddy Current Brake System for Detumbling Malfunctioning Satellites," in *Proc. IEEE/SICE Int. Symp. on System Integration*, 2012.

[2] L. Anselmo, et al., "Analysis of the consequences in low Earth orbit of the collision between Cosmos 2251 and Iridium 33," in *Proc. 21st Int. Symp. on Space Flight Dynamics*, 2009.

[3] M. Oda et al., "ETS-VII, space robot in-orbit experiment satellite," in *Proc. IEEE Int. Conf. on Robotics and Automation*, 1996, pp. 739–744.

[4] R. B. Friend, "Orbital express program summary and mission overview," in *Proc. of SPIE*, vol. 6958, 2008.

[5] R. P. Hoyt, et al., "The Terminator Tether: Autonomous Deorbit of LEO Spacecraft for Space Debris Mitigation," in *Proc. the 38th Aerospace Sciences Meeting & Exhibit*, 2000, pp. 10–13.

[6] S. Nishida et al., "Space debris removal system using a small satellite," *J. of Acta Astronautica*, vol. 65, no. 1, pp. 95–102, 2009.

[7] H. Kurosaki, et al., "Observation of Light Curve of GEO Debris etc.," in *Trans. of the Japan Society for Aeronautical and Space Sciences, Aerospace Technology Japan*, vol. 8, no. ists27, pp. Pr_2_63–Pr_2_68, 2010.

[8] S. Nakasuka, et al., "New method of capturing tumbling object in space and its control aspects," in *Proc. IEEE Int. Conf. Control Applications*, 1999, pp. 973–978.

[9] G. Rouleau, et al., "Autonomous capture of a tumbling satellite," in *Proc. of the IEEE Int. Conf. on Robotics and Automation*, 2006, pp. 3855–3860.

[10] S. Kawamoto, et al., "Ground experiment of mechanical impulse method for uncontrollable satellite capturing," *Proc. the 6th Int. Symp. on Artificial Intelligence and Robotics & Automation in Space* , 2001.

[11] S. Matunaga, et al., "Rotational motion-damper for the capture of an uncontrolled floating satellite," in *J. of Control Engineering Practice*, vol. 9, pp. 199–205, 2001.